



Published in final edited form as:

ACS Comb Sci. 2017 March 13; 19(3): 161–172. doi:10.1021/acscmbosci.6b00174.

Discovery of Peptidomimetic Ligands of EED as Allosteric Inhibitors of PRC2

Kimberly D. Barnash[†], Juliana The[‡], Jacqueline L. Norris-Drouin[†], Stephanie H. Cholensky[†], Beau M. Worley[†], Fengling Li[‡], Jacob I. Stuckey[†], Peter J. Brown[‡], Masoud Vedadi[‡], Cheryl H. Arrowsmith[‡], Stephen V. Frye^{*†}, and Lindsey I. James^{*†}

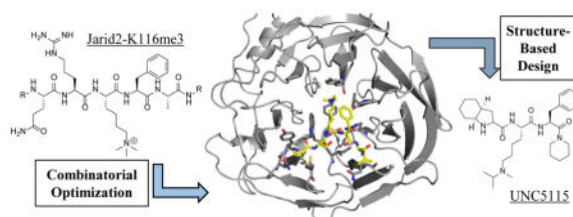
[†]Center for Integrative Chemical Biology and Drug Discovery, Division of Chemical Biology and Medicinal Chemistry, UNC Eshelman School of Pharmacy, University of North Carolina at Chapel Hill, Chapel Hill, North Carolina 27599, USA

[‡]Structural Genomics Consortium, University of Toronto, Toronto, Ontario, M5G 1L7, Canada

Abstract

The function of EED within Polycomb repressive complex 2 (PRC2) is mediated by a complex network of protein-protein interactions. Allosteric activation of PRC2 by binding of methylated proteins to embryonic ectoderm development (EED) aromatic cage is essential for full catalytic activity, but details of this regulation are not fully understood. EED's recognition of the product of PRC2 activity, histone H3 lysine 27 trimethylation (H3K27me3), stimulates PRC2 methyltransferase activity at adjacent nucleosomes leading to H3K27me3 propagation and, ultimately, gene repression. By coupling combinatorial chemistry and structure-based design, we optimized a low affinity methylated jumonji, AT rich interactive domain 2 (Jarid2) peptide to a smaller, more potent peptidomimetic ligand ($K_d = 1.14 \pm 0.14 \mu\text{M}$) of the aromatic cage of EED. Our strategy illustrates the effectiveness of applying combinatorial chemistry to achieve both ligand potency and property optimization. Furthermore, the resulting ligands, UNC5114 and UNC5115, demonstrate that targeted disruption of EED's reader function can lead to allosteric inhibition of PRC2 catalytic activity.

Graphical Abstract



Corresponding Authors: ingerman@email.unc.edu and svfrye@email.unc.edu.

The authors declare no competing financial interest.

Supporting Information. Supporting figures, a detailed description of the chemical synthesis and characterization, and the materials and experimental methods are described in the Supporting Information. This material is available free of charge via the Internet at <http://pubs.acs.org>.

Keywords

Methyl-lysine; Polycomb; one-bead-one-compound; peptidomimetic

INTRODUCTION

PRC2 is a multisubunit protein complex controlling cellular fate decisions through epigenetic transcriptional repression of key genes involved in development. The fundamental role of PRC2 deposition of the repressive chromatin mark, H3K27me₃, promoted extensive characterization of the PRC2 core complex, consisting of enhancer of zeste homolog 1/2 (Ezh1/2) (the methyltransferase catalytic subunit), suppressor of zeste 12 (Suz12), and EED¹⁻⁴. As a central mediator of gene repression, PRC2 functions are both diverse and essential, but the complexity of PRC2 biology has prevented the establishment of a straightforward and comprehensive model for its actions⁵⁻⁷. Recent efforts have led to new insights into PRC2 regulation of chromatin structure and gene repression along with indications of PRC2 misregulation in disease, particularly in cases of hematopoietic cancers⁸ and pediatric glioma⁹. The discovery of potent, *in vivo* chemical probes of Ezh1/2¹⁰⁻¹³ have aided in validating Ezh2 as a druggable component of PRC2, and encouragingly, Ezh2 inhibitors have since entered clinical trials¹⁴. New chemical tools to study other components of PRC2 may similarly provide a path to an improved understanding of its regulation, function, and therapeutic potential.

While a complete mechanistic understanding of PRC2 function remains elusive, several research groups have characterized the allosteric regulation of PRC2 activity facilitated by EED. Similar to many WD40 proteins, EED serves as a scaffold for protein complex assembly¹⁵. EED's indispensable role in PRC2 involves an intricate network of protein-protein interactions with both Ezh2 and Suz12, as Ezh2's catalytic activity is entirely dependent on PRC2 core complex formation³⁻⁴. EED associates with the product of PRC2 activity, H3K27me₃, and EED binding to H3K27me₃ stimulates PRC2 to methylate adjacent nucleosomes leading to H3K27me₃ propagation over large genomic loci and gene repression¹⁶. EED has also been shown to interact with inhibitory histone marks (histone H1 lysine 26 trimethylation)¹⁷, but the biological significance of this mark for EED regulation has been poorly studied.

Recently, Jarid2 trimethylated at lysine 116 (Jarid2-K116me₃) was described as an EED binding partner and allosteric activator of PRC2 methyltransferase activity¹⁸. The regulation of PRC2 through EED binding to both H3K27me₃ and Jarid2-K116me₃ illustrates the difficulty in developing a comprehensive model for PRC2 regulation. Moreover, the methylated Jarid2 peptide demonstrates 10-fold higher affinity for EED *in vitro* than H3K27me₃ (3.4 vs 40 μ M).

The recently solved crystal structures of the three core components of PRC2 are noteworthy achievements, and importantly provide a clear model for the allosteric activation of Ezh2's methyltransferase activity by EED^{15,19,20}. Engagement of the aromatic cage and top surface of EED by methylated Jarid2-K116me₃ (or H3K27me₃)¹⁵ stimulates the folding of an unstructured region of Ezh2 into an alpha helix, denoted as the stimulation response motif

(SRM). This helix in turn stabilizes the SET-I helix which forms part of the substrate binding site of the Ezh2 SET domain. Overall, these results suggest that EED ligands may either act as positive allosteric modulators of Ezh2, if they fully mimic natural ligands and aid in folding the SRM helix, or potentially act as inhibitors if they: bind and do not stabilize the SRM helix, thereby blocking allosteric activation by endogenous EED ligands (neutral allosteric interaction); or bind and also disrupt substrate binding in the orthosteric, catalytic site (negative allosteric modulators).²¹

There is a growing interest in targeting chromatin-modifying enzymes with small molecules, and inhibitors for methyl-lysine (Kme) readers are similarly desirable as tools to elucidate the role of these readers in chromatin dysregulation and disease^{22–23}. However, targeting the surface-groove binding mode of most Kme readers remains challenging, an issue exemplified by the dearth of chemical tools for studying Kme reader function. Currently, only two chemical probes of Kme readers have been published, while seven additional targets have literature on ligand development but lack adequate characterization, affinity, or cellular efficacy to be considered probes^{24–31}. Of the two successful chemical probes, the discovery of a peptide-derived chemical probe, UNC3866, for the Polycomb repressive complex 1 (PRC1) chromodomain Kme3 readers has demonstrated the potential for selectively targeting these readers via cell permeable peptide mimetics³². Utilizing peptides as a foundation for inhibitor discovery offers several advantages including a rational starting point based on the native ligand. Additionally, our recent development of a combinatorial peptide platform to target Kme reader proteins enables rapid peptide optimization²⁴. Such a combinatorial strategy for inhibitor discovery bypasses many of the drawbacks of a more traditional medicinal chemistry approach, namely cost, synthetic effort, and possible missed synergistic effects. Furthermore, compound libraries can be designed to improve ligand properties and competitor exchange kinetics can be applied to isolate ligands of equal or better potency. Thus, peptide ligand optimization provides an efficient and cost effective strategy for developing new chemical tools to study EED biology.

We present an *in vitro* chemical toolkit to study the role of EED's Kme reader function in the context of PRC2 activity. The pairing of combinatorial chemistry and structure-based design provides a platform for rapid optimization of ligand potency and chemical properties. This strategy enabled us to optimize the 12-mer Jarid2-K116me3 peptide to the 4-mer UNC5114, a 1 μ M EED binder. A biotinylated derivative effectively chemiprecipitated the core PRC2 components, EED, Suz12, and Ezh2, from cell lysates. Finally, we demonstrate that the targeted disruption of EED's reader function allosterically inhibits PRC2 catalytic activity. (While this manuscript was in revision a study reporting EED directed PRC2 inhibitors developed from an HTS hit appeared.³³)

METHODS

EED expression and purification (*Library screening, ITC, FP assays*)

The chromodomain of CBX7 (residues 8–65 of NP_055107) was expressed and purified as previously described³². Full length EED (reference sequence AAD08714) was expressed with an N-terminal His-tag in a pET28 vector. The pET28-EED expression construct was transformed into Rosetta2 BL21(DE3)pLysS competent cells (Novagen, EMD Chemicals,

San Diego, CA). Protein expression was induced by growing cells at 37°C with shaking until the OD₆₀₀ reached ~0.6–0.8 at which time the temperature was lowered to 15°C and expression was induced by adding 0.1mM IPTG and continuing shaking overnight. Cells were harvested by centrifugation and pellets were stored at –80°C.

His-tagged EED protein was purified by resuspending thawed cell pellets in 30ml of lysis buffer (50mM sodium phosphate pH 7.2, 150mM NaCl, 30mM imidazole, 1X EDTA free protease inhibitor cocktail (Roche Diagnostics, Indianapolis, IN)) per liter of culture. Cells were lysed on ice by sonication with a Branson Digital 450 Sonifier (Branson Ultrasonics, Danbury, CT) at 40% amplitude for 12 cycles with each cycle consisting of a 20 second pulse followed by a 40 second rest. The cell lysate was clarified by centrifugation and loaded onto a HisTrap FF column (GE Healthcare, Piscataway, NJ) that had been pre-equilibrated with 10 column volumes of binding buffer (50mM sodium phosphate pH 7.2, 500mM NaCl, 30mM imidazole) using an AKTA FPLC (GE Healthcare, Piscataway, NJ). The column was washed with 15 column volumes of binding buffer and protein was eluted in a linear gradient to 100% elution buffer (50mM sodium phosphate pH 7.2, 500mM NaCl, 500mM imidazole) over 20 column volumes. Peak EED containing fractions were pooled and concentrated to less than 8ml in Amicon Ultra-15 concentrators 10kDa molecular weight cut-off (Merck Millipore, Carrigtwohill Co. Cork IRL). Concentrated protein was loaded onto a HiLoad 26/60 Superdex 200 prep grade column (GE Healthcare, Piscataway, NJ) that had been preequilibrated with 1.2 column volumes of sizing buffer (25mM Tris pH 7.5, 500mM NaCl, 2mM DTT, 5% glycerol) using an AKTA FPLC (GE Healthcare, Piscataway, NJ). Protein was eluted isocratically in sizing buffer over 1.3 column volumes at a flow rate of 2ml/min collecting 3ml fractions. Peak fractions were analyzed for purity by SDS-PAGE and those containing pure protein were pooled and concentrated using Amicon Ultra-15 concentrators 10kDa molecular weight cut-off (Merck Millipore, Carrigtwohill Co. Cork IRL). Concentrated EED protein was dialyzed into a buffer containing 25mM Tris, pH 7.5, 250mM NaCl, 2mM DTT, 5% glycerol for storage.

Library Screening

For the first generation library, one-tenth of the synthesized library was removed to a 2 mL Eppendorf tube and equilibrated in 25 mM Tris, pH 7.8, 150 mM NaCl, and 0.1% Tween-20 (TBST) overnight. All incubation steps were conducted at room temperature. Individual magnetic screens follow a similar protocol to that originally described by Astle et al². For 1 hour, the beads were blocked in 5% BSA in TBST (1.8 mL). The resin was washed three times in TBST (1.8 mL) followed by addition of 1 μM His-tagged CBX7 (His6X-CBX7) in 2.5% BSA in TBST (1.8 mL) for 1 hour. Protein G Dynabeads (10 μL; Life Technologies) were loaded with mouse anti-His antibody (2 μL of a 1 μg/μL solution; Pierce MA1-21315) concurrently (1 hour). Excess antibody was removed and the Dynabeads were washed 3 times with TBST (200 μL), and the library was also washed 3 times with TBST (1.8 mL). A solution of the anti-His antibody loaded Dynabeads in 2.5% BSA in TBST (1.5 mL) was added to the library, and the library beads and magnetic beads were left to rotate for hour. A magnet was used to separate CBX7 hits and nonspecific binders from the remaining library. To prepare for the subsequent EED screen, the remaining library was stripped with 1% SDS (1.8 mL) at 95°C for 3 minutes. The library was then rinsed with 0.1% Tween-20, 1M

sodium chloride, and three times with TBST. The library was rotated in TBST overnight at 4°C. The next day 1 μM His6X-EED was screened as described above except magnetized hits from this screen were isolated and saved in a 0.6 mL Eppendorf tube. Hit PEGA beads were left to settle at the bottom of the tube while excess magnetic beads were removed by pulling off the solution by pipette. A solution of 10 μM Jarid2_{114–118}K116me3 in 2.5% BSA in TBST (500 μM) was added to the hit beads. The hits were left to rotate in this solution for 2 hours, and the beads were subjected to a magnet and unmagnetized beads were removed to a separate Eppendorf tube. The hit beads that remained magnetized throughout the soluble competitor treatment were stripped with 1% SDS at 95°C for 3 minutes then rinsed repeatedly with TBST followed by 0.1% Tween-20 and finally rinsed and equilibrated overnight in ethanol.

The second generation library also employed a negative selection (His6X-CBX7) and target screening (His6X-EED) as described above, except 20 μL Protein G Dynabeads was used with 4 μL of anti-His antibody. Compound 2 was used as the soluble competitor.

FP Assays

Binding assays were carried out in buffer containing 20 mM Tris (pH 7.5), 150 mM NaCl, and 1mM CHAPS in black 384-well microplates (Greiner) with total reaction volumes of 25 μL . To each well, 15 μL of buffer was added followed by the addition of 5 μL of a 2,000, 1,000, 0.500, 0.250, and 0.125 μM compound 3-FAM. Serial dilutions of His6x-EED were prepared and 5 μL was added to give final protein concentrations ranging from 0–50 μM . After 30 minutes at room temperature, FP measurements were taken on an AcQuest (LJL BioSystems) plate reader, with an excitation wavelength of 485 nm and the emission collected at 530 nm. This 2D titration was run in duplicate and led to the selection of 50 nM of compound 3-FAM and 1.5 μM of His6xEED as concentrations for follow-up displacement assays since. This combination was selected due to approximately 80% saturation of EED binding sites and a significant signal-to-noise window.

Displacement assays were conducted similarly, but with the following changes. First, 10 μL of buffer was added before addition of 5 μL of 0.250 compound 3-FAM and 5 μL of 7.5 μM His6x-EED. After 30 minutes, 5 μL from serial dilutions (0–100 μM) of each compound were added to the wells. The plate was left to incubate at room temperature for an additional 30 minutes and then read. Each reaction was run in triplicate or quadruplicate.

ITC Experiments

ITC measurements were recorded at 25°C using an AutoITC200 microcalorimeter (MicroCal Inc., MA). Protein stocks were prepared in ITC buffer (25 mM Tris-HCl, pH 8, 250 mM NaCl, and 2 mM β -mercaptoethanol) and then diluted into ITC buffer to achieve a final concentration of 50 μM (325 μL). All compounds were dissolved in water to a stock concentration of 10 mM and then diluted to a final concentration of 500 μM . A typical experiment included a single 0.2 μL compound injection into a 200 μL cell filled with protein, followed by 26 subsequent 1.5 μL injections of compound. Injections were performed with a spacing of 180 s and a reference power of 8 $\mu\text{cal/s}$. The titration data was analyzed using Origin Software (MicroCal Inc., USA) by nonlinear least-squares, fitting the heats of

binding as a function of the compound:protein ratio to a one site binding model. The first data point was deleted from all analyses.

PRC2 Complex Expression and Purification

DNA fragments encoding the genes of the full lengths of two components of PRC2 complex, EED(1–441) and EZH2(1–751) were cloned into pFastBac-Dual (Invitrogen) and the full length of SUZ12(1–739) were cloned into pFastBac HT A (Invitrogen). The resulting plasmids were transformed into DH10Bac™ Competent *E. coli* (Invitrogen) and the recombinant viral DNA bacmids were purified and followed by a recombinant baculovirus generation in Sf9 insect cells. Sf9 cells grown in HyQ®SFX insect serum-free medium (ThermoScientific) were co- infected with 10 ml of each P3 viral stocks per 0.8 L of suspension cell culture and incubated at 27°C using a platform shaker set at 100 RPM. The cells were collected after 72 hours of post infection time, when viability dropped to 70–80%. Harvested cells were re-suspended in PBS, 1X protease inhibitor cocktail (2.5 µg/ml Aprotinin, 2.5 µg/ml Leupeptin, 2.5 µg/ml Pepstatin A and 2.5 µg/ml E-64) or a complete EDTA-free protease inhibitor cocktail tablet (Roche). The cells were lysed chemically by rotating 30 min with NP-40 (final concentration of 0.6%) and 50 U/mL Benzonase nuclease (Sigma) and 2 mM 2-mercaptoethanol followed by sonication at frequency of 8 (10 sec on/10 sec off) for 4 min (Sonicator 3000, Misoni). The crude extract was clarified by high-speed centrifugation (60 min at 36,000 ×g at 4°C) in a Beckman Coulter centrifuge. The recombinant protein complex was purified by incubating the cleared lysate with equilibrated Anti-FLAG M2 Affinity agarose gel (Sigma, Cat # A2220) for 1.5 hours with rotating, followed by washing with 10 column volumes of TBS (50 mM Tris-HCl, with 150 mM NaCl, pH 7.4). The recombinant protein complex was eluted by competitive elution with 100 µg/ml FLAG peptide (Sigma, Catalog # F4799) in TBS and 5% glycerol. Purity was judged by SDS–PAGE and the protein was subsequently concentrated and flash frozen. Aromatic cage mutations of EED in this PRC2 construct were also created by site-directed mutagenesis as described for the EED single constructs. PRC2 complexes containing these EED mutations were expressed and purified as the wildtype.

PRC2 Methyltransferase Activity Assay

Methyltransferase activity assays for EZH2 trimeric complex (EZH2:EED:SUZ12) were performed by monitoring the incorporation of tritium-labeled methyl group to lysine 27 of H3 (21–44) peptide using Scintillation Proximity Assay (SPA). The enzymatic reactions were performed at 23 °C with 1 hour incubation of 10 µl reaction mixture in 20 mM Tris-HCl, pH 8, 5 mM DTT, and 0.01% Triton X-100 containing 1 µM of ³H-SAM (Cat.# NET155V250UC; Perkin Elmer; www.perkinelmer.com), 1 µM of biotinylated H3 (21–44), 20 nM EZH2 complex, and compound titration from 50 µM to 50 µM. To stop the reactions, 10 µL of 7.5 M Guanidine hydrochloride was added, followed by 200 µl of buffer (20 mM Tris, pH 8.0), mixed and transferred to a 96-well Streptavidin coated Flash-plate (PerkinElmer, <http://www.perkinelmer.ca>). After mixing, Flash-plates were incubated for 2 hour and the CPM counts were measured using Topcount plate reader (Perkin Elmer, www.perkinelmer.com). The CPM counts in the absence of compound for each dataset were defined as 100% activity. In the absence of the enzyme, the CPM counts in each data set were defined as background (0%). All enzymatic reactions were performed in triplicate and

IC₅₀ values were determined by fitting the data to Four Parameter Logistic equation using GraphPad Prism 7 software.

For competition experiments with H3K27me3 peptide, 0, 1 or 10 μM H3K27me3 (19–33) peptide were included in the reaction mixture. For data sets involving comparison of the wildtype complex activity against those of the mutants, the CPM counts of the wildtype complex in the absence of compound were defined as 100% activity. In the absence of the enzyme, the CPM counts in each data set were defined as background (0%). The enzymatic reactions were performed in triplicate and IC₅₀ values were determined by fitting the data to Four-Parameter Logistic equation using SigmaPlot version 11.0.

Additional methods, including compound synthesis and characterization, crystallography, and pull-down experiments, are described in the Supporting Information.

RESULTS AND DISCUSSION

The recent characterization of EED's binding to methylated Jarid2 at low micromolar potency (Jarid2_{110–120}-K116me3, $K_d \sim 3 \mu\text{M}$)¹⁸ provided a rational starting point for peptide optimization to target the reader interface of EED. We initially set out to design and test the affinity of a truncated Jarid2-K116me3 peptide. By analyzing the co-crystal structure of Jarid2-K116me3 and EED (PDB 4X3E) we noted that the majority of specific protein-protein contacts were largely confined to five residues within Jarid2 (Jarid2_{114–118}-K116me3, Figure 1a). Distinctively, the glutamine 114 side chain rests in a small hydrophobic pocket while the backbone carbonyl appears to make a hydrogen bond with tryptophan 364 of the EED aromatic cage. K116me3 binds in the aromatic cage while its carbonyl and that of the adjacent arginine 115 form additional hydrogen bonds with EED. Unlike the H3K27 sequence, Jarid2_{114–118}-K116me3 contains a phenylalanine at the +1 position adjacent to the methylated lysine. Phenylalanine 117 was shown to be essential for Jarid2 binding and the crystal structure demonstrates that the aromatic ring is positioned to either stack with phenylalanine 97 of the aromatic cage or to further enclose K116me3 within the cage. Lastly, alanine 118 of Jarid2 binds in a shallow hydrophobic patch on EED's surface. We synthesized Jarid2_{114–118}-K116me3 and tested its affinity for EED by isothermal titration calorimetry (ITC) ($K_d = 8.82 \pm 2.06 \mu\text{M}$; Supplementary Information Figure S1). The truncated peptide demonstrated less than a 3-fold loss in affinity compared to the published value for Jarid2_{110–120}-K116me3, confirming that the bulk of EED's affinity for Jarid2-K116me3 is due to contacts with these five residues.

To confirm EED's compatibility with our on-bead, magnetic enrichment screening approach (Figure 1b), Jarid2_{114–121}-K116me3 was synthesized on PEGA resin (Jarid2_{114–121}-K116me3-PEGA) as a control ligand^{24,34}. Histone peptides, with their high charge density and numerous arginines, lysines and glutamines, interact non-specifically with the components of the on-bead assay. The longer Jarid2 peptide seemed likely to face similar issues, which led us to select a truncated Jarid2 peptide sequence for on-bead screen development. Though the longer peptide is unnecessary for maintaining affinity to EED, the additional residues serve as a spacer between the methionine required for cyanogen bromide (CNBr) cleavage and the protein-binding region of the peptide. Following our previous Kme

reader screening protocol²⁴, His-tagged EED (His6X-EED) was incubated with bovine serum albumin-blocked Jarid2₁₁₄₋₁₂₁-K116me3-PEGA. Simultaneously, mouse anti-His6X antibody was bound to magnetic Protein G Dynabeads. Following extensive washing, the antibody-coated Dynabeads were added to the preincubated Jarid2₁₁₄₋₁₂₁-K116me3-PEGA resin. Jarid2₁₁₄₋₁₂₁-K116me3-PEGA became selectively magnetized only in the presence of His6X-EED, as expected. In contrast, UNC3866-PEGA failed to become magnetized in either the presence or absence of His6X-EED which recapitulated EED's lack of affinity for UNC3866 in solution-based assays³² and helped to confirm that successful magnetization occurs only in the presence of genuine EED ligands.

Having established the peptide region of Jarid2 that we planned to optimize and validated EED in our magnetic enrichment assay, we began designing a first generation combinatorial library of potential EED ligands (Figure 1c). Our initial library design focused on improving the undesirable properties of Jarid2₁₁₄₋₁₁₈K116me3, namely the presence of a primary amine at the N-terminus, a quaternary amine, a guanidinyll group, and an overall +3 charge state. Our library tested a variety of carboxylic acid caps at the N-terminus as replacements for glutamine 114, while also including an acetyl-capped glutamine in case this residue was required for EED activity. Previous studies indicated that an arginine at the -1 position of Kme3 was essential for stimulation of PRC2 catalytic activity though unnecessary for binding to EED¹⁶⁻¹⁷. Potential arginine replacements in our library included serine and alanine, for example, as well as riskier substitutions including peptoid residues in an attempt to reduce the number of backbone hydrogen bond donors. A variety of natural and unnatural aromatic residues were tested in place of Phe at the R4 position, while only modest changes were included at the Kme3 position.

Using split-and-pool synthesis³⁵, the 1,029 compound library was synthesized at approximately 20-fold redundancy (Figure 1c). To diminish the resynthesis of false positives we included multiple copies of each potential ligand in the library so that hits could be prioritized by redundancy for follow-up studies³⁶. Kme derivatives were synthesized via reductive amination with lysine to form the tertiary amines followed by substitution to yield the desired quaternary amines. Incorporation of methionine as the first residue of the linker enabled cyanogen bromide (CNBr) cleavage from the resin for hit deconvolution by MALDI MS/MS. Amino acids were added via standard Fmoc solid phase synthesis while peptoids were synthesized by bromoacetic acid coupling and then substitution with a primary amine. Deprotection of the pooled library to remove Boc/tBu groups was conducted under acidic conditions, and then the final library was equilibrated in aqueous buffer prior to screening.

A preliminary negative selection of the library was conducted with the chromodomain of CBX7, a Kme reader also known to bind H3K27me3. Magnetized beads were presumed to either bind nonspecifically to the components of the assay (Protein G Dynabeads and anti-His6x antibody) or specifically to CBX7. Magnetized beads were removed from the library while the unmagnetized beads were carried forward, and His6X-EED was then screened against the remaining library. Magnetically isolated EED hit beads were separated and treated with a soluble competitor ligand, Jarid2₁₁₄₋₁₁₈K116me3 (10 μ M), to elute off low affinity hits and retain only those ligands with improved potency over the truncated Jarid2

peptide. After 120 minutes, those hits that remained magnetized were isolated, stripped, and cleaved from the bead with CNBr before being sequenced by tandem mass spectrometry.

Two hits were isolated with a greater than 2-fold redundancy (Figure 1d; Supplementary Information Figure S2), both of which included cyclohexane carboxylic acid as a glutamine replacement at the N-terminus. At positions R4 and R3, respectively, phenylalanine and Kme3 residues were conserved, but the hits varied at the R2 position containing either a lysine or serine. After resynthesis of compound **1**, hit confirmation by ITC demonstrated a slight improvement in potency relative to Jarid₂₁₁₄₋₁₁₈K116me3 (compound **1**: $K_d = 4.74 \pm 0.69 \mu\text{M}$ vs Jarid₂₁₁₄₋₁₁₈K116me3: $K_d = 8.82 \pm 2.06 \mu\text{M}$; Supplementary Information Figure S1). In addition to replacing the N-terminal amine and the glutamine side chain primary amide, both ligands also revealed suitable replacements for the guanidinyll group of arginine. Overall, this first generation EED-targeted library resulted in improved ligand potency and physicochemical properties while important insights were gained into the amenability of replacing the two N-terminal residues.

We next designed a larger second generation library consisting of 4,410 compounds taking into account insights from our initial screening results (Figure 2). The goal of this library was primarily to improve ligand affinity so both conservative and riskier modifications were tested at positions R1, R2, R4, and R5 while only Kme3 was incorporated at position R3. For instance, several phenylalanine derivatives were included at position R4 to potentially improve the interaction of the ring with the aromatic cage or the Kme3 side chain. We included a deeper exploration of cyclic analogs at the N-terminal capping position based on conservation of the cyclohexyl cap in both hits of the first generation library. Additionally, while the C-terminal alanine was not altered in the previous library, a variety of residues with small hydrophobic side chains were included in the second generation library to probe a small hydrophobic patch on EED's surface. Additionally, the second generation library included a modified linker. Firstly, an alkyne was included because previous studies³⁷⁻³⁸ had applied this strategy to derivatize ligands after bead cleavage, though our approach in this study did not employ this group. Secondly, alanine and beta-alanine were included in the linker to provide space between the compound and the methionine and the alkyne. Since this library sought only to probe the affinity of the 5-mer peptide, the native sequence was not used as the linker to avoid any effects this sequence might have on affinity.

Screening followed an identical protocol as described above with the substitution of compound **2** as the soluble competitor. Nine ligands with a redundancy greater than 2-fold were isolated, and a number of structural similarities were observed (a subset are shown in Supplementary Information Figure S3). The capping residue (R1) favored aliphatic heterocycles while significant tolerance was found at the R2 position. Although two hits with 3-fluorophenylalanine at R4 were identified, retention of phenylalanine was clearly preferred. Lastly, the R5 position favored either leucine or valine suggesting that increased hydrophobic contacts at the C-terminus improve the interaction between the peptide and EED. Based on these hit structures, we synthesized a peptide combining the residues that appeared most frequently (compound **3**; $K_d = 1.09 \pm 0.27 \mu\text{M}$; Supplementary Information Figure S1) which resulted in an approximately 4-fold enhancement in affinity compared to compound **1** (Figure 3a). By applying combinatorial optimization to Jarid₂₁₁₄₋₁₁₈K116me3,

only two iterations of library design and screening reduced the overall ligand charge from +3 to +2 and produced a 10-fold improvement in potency.

We next solved the co-crystal structure of compound **3** bound to EED (Figure 3b, (PDB 5TTW)). Unsurprisingly, the Kme3 and phenylalanine residues adopt an identical binding mode to Jarid2K116me3 (PDB 4X3E). Interestingly, the C-terminus binds in a unique orientation that positions the hydrophobic leucine side group toward EED's surface (Figure 3c,d). The isoleucine 363 side chain and the carbon chain of glutamine 382 form van der Waal contacts with the leucine side chain of **3** while the backbone primary amide does not interact with EED. Although the amide bond between phenylalanine and leucine in compound **3** does not appear to make specific hydrogen bond contacts, the carbonyls of lysine and serine form hydrogen bonds with residues at the base of EED's aromatic cage. Additionally, while the serine backbone seems critical for bridging the methylated lysine within the aromatic cage and the proline that interacts with a small hydrophobic pocket formed by asparagine 307, tyrosine 308, and cysteine 324, the side chain of serine has no apparent interactions, suggesting this group is non-essential for binding. This is consistent with the variability observed at this position in both libraries. Overall, the co-crystal structure strongly implicated the potential for replacing the leucine of compound **3** with a non-peptidic, hydrophobic group and replacement of the proline-serine N-terminus.

In the next phase of optimization, we C-terminally labeled compound **3** with fluorescein to enable an EED fluorescence polarization (FP) assay (Supplementary Information Figure S4a). Following optimization of protein and fluorescent ligand concentrations (Supplementary Information Figure S4b), we validated this assay by displacing the bait peptide with compound **3**, and an IC_{50} ($1.65 \pm 0.66 \mu\text{M}$) approximately the same as the K_d ($1.09 \pm 0.27 \mu\text{M}$) was observed (Table 1; curves shown in Supplementary Information Figure S5). Similarly, Jarid2₁₁₄₋₁₁₈K116me3 demonstrated an IC_{50} ($14.78 \pm 2.24 \mu\text{M}$) on par with its measured K_d ($8.82 \pm 2.06 \mu\text{M}$) so we moved forward by testing new compounds via FP followed by ITC characterization for the most promising ligands.

Subsequent compound optimization focused on modifying the two termini to reduce the length of the peptide and replacing the quaternary amine. Initially, the C-terminal leucine was replaced by a piperidinyl ring (compound **4**). This substitution had minimal effects on potency indicating that the piperidine ring could mimic important hydrophobic contacts made by the leucine side chain while both the C-terminal amide and the backbone amide proton of the leucine residue were not required for EED binding. Next, since quaternary amines are suggested to prevent passive diffusion through the lipid bilayer, the trimethyl substitution on the lysine was replaced by various tertiary amines including diethyl (**5**), methyl-cyclohexyl (**6**), and methyl-isopropyl (**7**). When compared to Kme3, the corresponding methyl-cyclohexyl ligand lost nearly all binding to EED ($IC_{50} > 30 \mu\text{M}$) whereas the diethyl-lysine-containing ligand resulted in a 7-fold reduction in potency. Methyl-isopropyl was found to be the best substitute for Kme3 with only a 3-fold loss in affinity. Following selection of methyl-isopropyl lysine (Kme,iPr) for further optimization, three bicyclic capping residues were tested to replace the proline-serine N-terminus. While two of the capping residues containing aromatic rings to potentially stack with tryptophan 364 or tyrosine 308 did not potently interact with EED (compounds **8** and **9**), an (2S,3aS,

7aS)-octahydro-1H-indole cap (compound **10**, UNC5114) not only maintained EED affinity but even compensated for the slight loss in potency due to the Kme,iPr substitution. Incorporating the C-terminal piperidiny ring into UNC5114 (compound **11**, UNC5115) resulted in a 2-fold loss in potency relative to UNC5114. Follow-up ITC experiments confirmed UNC5114 ($K_d = 0.68 \pm 0.05$) and UNC5115 ($K_d = 1.14 \pm 0.14$) potencies. Additionally, we speculated that methylation of the phenylalanine amide in UNC5115 would disrupt the ability of the phenyl ring to fold over the aromatic cage and the lysine side chain, thus abolishing EED binding. UNC5197 (Figure 4a) ITC data confirmed that this methylation disrupts binding and hence this compound represents an ideal negative control for subsequent studies. Overall, UNC5114 contains only three hydrogen bond donors and a +2 charge state which is a dramatic improvement over the 5-mer Jarid2₁₁₄₋₁₁₈K116me3 ligand that includes nine hydrogen bond donors and a +3 charge state.

Having discovered of a set of peptide-competitive chemical tools with low micromolar to high nanomolar *in vitro* affinities for EED, we next sought to investigate how targeted disruption of the PRC2 reader function would alter catalytic activity of the complex. Although previous studies have demonstrated allosteric activation of PRC2 catalytic activity by several methylated peptides, we hypothesized that our ligands would not be stimulatory because they lack the requisite arginine at the -1 position to Kme3 that is required for stabilization of the SRM helix. We moved forward by characterizing the effects of compound **3**, UNC5114, and UNC5115 in a PRC2 methyltransferase scintillation proximity assay¹² (Figure 4b). In brief, this assay monitors the transfer of a tritiated methyl group from the cofactor S-adenosyl methionine to a histone H3₂₁₋₄₄K27 unmodified peptide. Interestingly, all three ligands inhibit catalytic activity, albeit to only about 80% at saturating concentrations of ligand. We believe this residual 20% activity may correspond to a basal activity of the unstimulated Ezh2 enzyme within the PRC2 core complex, as direct inhibition of Ezh2 catalytic domain with SAM-competitive inhibitors completely eliminates enzyme activity^{10,11,12,13}.

To biochemically probe the allosteric inhibition of PRC2 via binding to the EED reader pocket, UNC5114 and UNC5115 were incubated with the PRC2 core complex in the presence or absence of the stimulatory H3K27me3 peptide. Increasing concentrations of the H3K27me3 peptide increased the activity of the enzyme but also increased the apparent IC₅₀ values of both compounds (Figure 5). These results are consistent with a mechanism of action in which the compounds inhibit PRC2 by competing with the stimulatory peptide, thereby preventing allosteric stimulation of the enzyme. EED aromatic cage mutants (F97A, W364A, and Y365A) were also generated to further test this mechanism of PRC2 inhibition. Differential static light scattering (DSLS) confirmed that all three mutants demonstrated a similar thermal aggregation stability profile to wild-type EED, suggesting that these mutants are properly folded (Supporting Information Figure S6). When reconstituted into a core PRC2 complex, the EED mutants exhibit significantly lower levels of basal catalytic activity, and UNC5114 and UNC5115 clearly fail to inhibit this activity whereas the EZH2 chemical probe UNC1999 completely abrogates the activity (Supporting Information Figure S7), similar to its inhibition of wildtype PRC2. Taken together, these results demonstrate that

UNC5114 and UNC5115 act as allosteric inhibitors of PRC2 methyltransferase activity through competitive inhibition of the EED Kme reader function.

In order to confirm that UNC5114 and UNC5115 are able to target native PRC2 from cells, we biotinylated UNC5114 to attempt chemiprecipitation of PRC2 components from cellular lysates (Figure 6a). Streptavidin coated magnetic Dynabeads were incubated with biotinylated UNC5114 followed by the addition of PC-3 cell lysates in the presence and absence of soluble UNC5114 to confirm the specificity of the pulldown. Western blot analysis indicated successful pulldown of all three core components of PRC2: EED, Ezh2, and Suz12 (Figure 6b). These results confirm that biotin-UNC5114 engages the Kme reader pocket of EED without disrupting assembly of the PRC2 complex and that our ligands bind endogenous EED.

CONCLUSIONS

A paired combinatorial and structure-based optimization strategy led to the discovery of two small, peptidomimetic ligands of EED. These ligands exhibit improved potency (~10-fold) and physicochemical properties compared to Jarid2₁₁₄₋₁₁₈K116me3, and they demonstrate the feasibility of optimizing a peptidic antagonist of a Kme reader domain for targeted disruption of its reader function. Moreover, compound **3** could be easily functionalized to facilitate the development of an FP assay, and UNC5114-biotin enabled chemiprecipitation experiments that show maintenance of affinity for endogenous EED. Most interestingly, the disruption of PRC2 catalytic activity by UNC5114 and UNC5115 presents a unique opportunity to probe allosteric regulation of H3K27me3 deposition particularly when considering that the allosteric mechanisms governing PRC2 are only beginning to be understood. It is possible that, in addition to competitively preventing allosteric activation, these peptidomimetic EED ligands disrupt catalytic activity by preventing the stabilization and orientation of the stimulation response motif (SRM) helix of EZH2 as described by Jiao and Liu¹⁵ (Figure 7). Consequently, the SRM helix cannot in turn stabilize the SET-I helix which contributes many of the residues that interact with the substrate peptide, as required for more efficient catalytic activity. Further dissection of this mechanism and determination of whether these ligands are neutral allosteric modulators or negative allosteric modulators will depend upon definition of the structural changes in PRC2 upon binding of these compounds.²¹ Ultimately, these ligands recapitulate the centrality of EED to the catalytic output of PRC2.

Supplementary Material

Refer to Web version on PubMed Central for supplementary material.

Acknowledgments

We thank N. Dicheva and the UNC Michael Hooker Proteomics Center for assistance with and use of their AbSciex 5800 MALDI-TOF/TOF. The authors acknowledge M. Ravichandran, S. Duan, and T. Hajian for EED mutant constructs and assistance with protein purification, and W. Tempel for reviewing crystallography data. The research described here was supported by the National Institute of General Medical Sciences, U.S. National Institutes of Health (NIH, grant R01GM100919) and the University Cancer Research Fund, University of North Carolina at Chapel Hill. The SGC is a registered charity (number 1097737) that receives funds from AbbVie, Bayer Pharma AG, Boehringer Ingelheim, Canada Foundation for Innovation, Eshelman Institute for Innovation, Genome Canada,

Innovative Medicines Initiative (EU/EFPIA) [ULTRA-DD grant no. 115766], Janssen, Merck & Co., Novartis Pharma AG, Ontario Ministry of Economic Development and Innovation, Pfizer, São Paulo Research Foundation-FAPESP, Takeda, and the Wellcome Trust.

ABBREVIATIONS

EED

embryonic ectoderm development

PRC2

Polycomb repressive complex 2

H3K27me3

histone H3 lysine 27 trimethylation

 K_d

dissociation constant

Jarid2

Jumonji/ARID domain-containing protein 2

Ezh1/2

enhancer of zeste homolog 1/2; suppressor of zeste 12 protein homolog

RbAp46/48

retinoblastoma-binding protein 46/48

H1K26me3

histone H1 lysine 26 trimethylation

Jarid2-K116me3

Jarid2 trimethylated at lysine 116

SRM

stimulation response motif

SET

Su(var) and 'Enhancer of zeste' proteins

SET-I

SET inhibitory

PRC1

Polycomb repressive complex 1

Kme

methyl-lysine

Jarid2₁₁₀₋₁₂₀-K116me3

Jarid2 peptide residues 110–120 trimethylated lysine 116me3

Jarid2_{114–118}K116me3

Jarid2 peptide residues 114–118 trimethylated lysine 116me3

ITC

isothermal titration calorimetry

His6X-EED

His-tagged EED

CNBr

cyanogen bromide

CBX7

chromobox protein homolog 7

FP

fluorescence polarization

IC₅₀

half maximal inhibitory concentration

iPr

isopropyl

References

1. Cao R, Wang L, Wang H, Xia L, Erdjument-Bromage H, Tempst P, Jones RS, Zhang Y. Role of Histone H3 Lysine 27 Methylation in Polycomb-Group Silencing. *Science*. 2002; 298(5595):1039–1043. [PubMed: 12351676]
2. Varambally S, Dhanasekaran SM, Zhou M, Barrette TR, Kumar-Sinha C, Sanda MG, Ghosh D, Pienta KJ, Sewalt RG, Otte AP. The polycomb group protein EZH2 is involved in progression of prostate cancer. *Nature*. 2002; 419(6907):624–629. [PubMed: 12374981]
3. Pasini D, Bracken AP, Jensen MR, Denchi EL, Helin K. Suz12 is essential for mouse development and for EZH2 histone methyltransferase activity. *The EMBO journal*. 2004; 23(20):4061–4071. [PubMed: 15385962]
4. Montgomery ND, Yee D, Chen A, Kalantry S, Chamberlain SJ, Otte AP, Magnuson T. The Murine Polycomb Group Protein Eed Is Required for Global Histone H3 Lysine-27 Methylation. *Curr Biol*. 2005; 15(10):942–947. [PubMed: 15916951]
5. Margueron R, Reinberg D. The Polycomb complex PRC2 and its mark in life. *Nature*. 2011; 469(7330):343–349. [PubMed: 21248841]
6. Aranda S, Mas G, Di Croce L. Regulation of gene transcription by Polycomb proteins. *Sci Adv*. 2015; 1(11):e1500737. [PubMed: 26665172]
7. Conway E, Healy E, Bracken AP. PRC2 mediated H3K27 methylations in cellular identity and cancer. *Curr Opin Cell Biol*. 2015; 37:42–48. [PubMed: 26497635]
8. Lund K, Adams PD, Copland M. EZH2 in normal and malignant hematopoiesis. *Leukemia*. 2014; 28(1):44–49. [PubMed: 24097338]
9. Lewis PW, Müller MM, Koletsky MS, Cordero F, Lin S, Banaszynski LA, Garcia BA, Muir TW, Becher OJ, Allis CD. Inhibition of PRC2 activity by a gain-of-function H3 mutation found in pediatric glioblastoma. *Science*. 2013; 340(6134):857–861. [PubMed: 23539183]
10. McCabe MT, Ott HM, Ganji G, Korenchuk S, Thompson C, Van Aller GS, Liu Y, Graves AP, Diaz E, LaFrance LV. EZH2 inhibition as a therapeutic strategy for lymphoma with EZH2-activating mutations. *Nature*. 2012; 492(7427):108–112. [PubMed: 23051747]

11. Qi W, Chan H, Teng L, Li L, Chuai S, Zhang R, Zeng J, Li M, Fan H, Lin Y, Gu J, Ardayfio O, Zhang JH, Yan X, Fang J, Mi Y, Zhang M, Zhou T, Feng G, Chen Z, Li G, Yang T, Zhao K, Liu X, Yu Z, Lu CX, Atadja P, Li E. Selective inhibition of Ezh2 by a small molecule inhibitor blocks tumor cells proliferation. *P Natl Acad Sci USA*. 2012; 109(52):21360–5.
12. Konze KD, Ma A, Li F, Barsyte-Lovejoy D, Parton T, MacNevin CJ, Liu F, Gao C, Huang X-P, Kuznetsova E. An orally bioavailable chemical probe of the lysine methyltransferases EZH2 and EZH1. *ACS Chem Biol*. 2013; 8(6):1324–1334. [PubMed: 23614352]
13. Campbell JE, Kuntz KW, Knutson SK, Warholc NM, Keilhack H, Wigle TJ, Raimondi A, Klaus CR, Rioux N, Yokoi A. EPZ011989, a potent, orally-available EZH2 inhibitor with robust in vivo activity. *ACS Med Chem Lett*. 2015; 6(5):491–495. [PubMed: 26005520]
14. Kim KH, Roberts CW. Targeting EZH2 in cancer. *Nature medicine*. 2016; 22(2):128–134.
15. Jiao L, Liu X. Structural basis of histone H3K27 trimethylation by an active polycomb repressive complex 2. *Science*. 2015; 350(6258)
16. Margueron R, Justin N, Ohno K, Sharpe ML, Son J, Drury WJ III, Voigt P, Martin SR, Taylor WR, De Marco V, Pirrotta V, Reinberg D, Gambin SJ. Role of the polycomb protein EED in the propagation of repressive histone marks. *Nature*. 2009; 461(7265):762–767. [PubMed: 19767730]
17. Xu C, Bian C, Yang W, Galka M, Ouyang H, Chen C, Qiu W, Liu H, Jones AE, MacKenzie F, Pan P, Li SS-C, Wang H, Min J. Binding of different histone marks differentially regulates the activity and specificity of polycomb repressive complex 2 (PRC2). *P Natl Acad Sci USA*. 2010; 107(45):19266–19271.
18. Sanulli S, Justin N, Teissandier A, Ancelin K, Portoso M, Caron M, Michaud A, Lombard B, Da Rocha ST, Offer J. Jarid2 methylation via the PRC2 complex regulates H3K27me3 deposition during cell differentiation. *Mol Cell*. 2015; 57(5):769–783. [PubMed: 25620564]
19. Justin N. Structural basis of oncogenic histone H3K27M inhibition of human polycomb repressive complex 2. *Nat Comm*. 7:11316.
20. Brooun A, Gajiwala KS, Deng Y-L, Liu W, Bolaños B, Bingham P, He Y-A, Diehl W, Grable N, Kung P-P. Polycomb repressive complex 2 structure with inhibitor reveals a mechanism of activation and drug resistance. *Nat Comm*. 2016:7.
21. Christopoulos A, Changeux J-P, Catterall WA, Fabbro D, Burris TP, Cidowski JA, Olsen RW, Peters JA, Neubig RR, Pin J-P, Sexton PM, Kenakin TP, Ehlert FJ, Spedding M, Langmead CJ. International Union of Basic and Clinical Pharmacology. XC. Multisite Pharmacology: Recommendations for the Nomenclature of Receptor Allosterism and Allosteric Ligands. *Pharmacol Rev*. 2014; 66(4):918. [PubMed: 25026896]
22. Frye SV, Heightman T, Jin J. Targeting methyl lysine. *Annu Rep Med Chem*. 2010; 45:329–343.
23. Arrowsmith CH, Bountra C, Fish PV, Lee K, Schapira M. Epigenetic protein families: a new frontier for drug discovery. *Nat Rev Drug Discov*. 2012; 11(5):384–400. [PubMed: 22498752]
24. Barnash KD, Lamb KN, Stuckey JI, Norris JL, Cholensky SH, Kireev DB, Frye SV, James LI. Chromodomain Ligand Optimization via Target-Class Directed Combinatorial Repurposing. *ACS Chem Biol*. 2016; 11(9):2475–2483. [PubMed: 27356154]
25. Herold JM, James LI, Korboukh VK, Gao C, Coil KE, Bua DJ, Norris JL, Kireev DB, Brown PJ, Jin J. Structure–activity relationships of methyl-lysine reader antagonists. *MedChemComm*. 2012; 3(1):45–51.
26. Miller TC, Rutherford TJ, Birchall K, Chugh J, Fiedler M, Bienz M. Competitive binding of a benzimidazole to the histone-binding pocket of the Pygo PHD finger. *ACS Chem Biol*. 2014; 9(12):2864–2874. [PubMed: 25323450]
27. Milosevich N, Gignac MC, McFarlane J, Simhadri C, Horvath S, Daze KD, Croft CS, Dheri A, Quon TT, Douglas SF. Selective Inhibition of CBX6: A Methyllysine Reader Protein in the Polycomb Family. *ACS Med Chem Lett*. 2015; 7(2):139–144. [PubMed: 26985288]
28. Perfetti MT, Baughman BM, Dickson BM, Mu Y, Cui G, Mader P, Dong A, Norris JL, Rothbart SB, Strahl BD. Identification of a fragment-like small molecule ligand for the methyl-lysine binding protein, 53BP1. *ACS Chem Biol*. 2015; 10(4):1072–1081. [PubMed: 25590533]
29. Ren C, Morohashi K, Plotnikov AN, Jakoncic J, Smith SG, Li J, Zeng L, Rodriguez Y, Stojanoff V, Walsh M. Small-molecule modulators of methyl-lysine binding for the CBX7 chromodomain. *Chem Biol*. 2015; 22(2):161–168. [PubMed: 25660273]

30. Wagner EK, Nath N, Flemming R, Feltenberger JB, Denu JM. Identification and characterization of small molecule inhibitors of a plant homeodomain finger. *Biochemistry*. 2012; 51(41):8293–8306. [PubMed: 22994852]
31. Wagner T, Greschik H, Burgahn T, Schmidtkunz K, Schott A-K, McMillan J, Baranauskien L, Xiong Y, Fedorov O, Jin J. Identification of a small-molecule ligand of the epigenetic reader protein Spindlin1 via a versatile screening platform. *Nucleic Acids Res*. 2016; 44(9):e88–e88. [PubMed: 26893353]
32. Stuckey JI, Dickson BM, Cheng N, Liu Y, Norris JL, Cholensky SH, Tempel W, Qin S, Huber KG, Sagum C. A cellular chemical probe targeting the chromodomains of Polycomb repressive complex 1. *Nature Chem Biol*. 2016; 12(3):180–187. [PubMed: 26807715]
33. Lingel A, Sendzik M, Huang Y, Shultz MD, Cantwell J, Dillon MP, Fu X, Fuller J, Gabriel T, Gu XJ, Jiang X, Li L, Liang F, McKenna MM, Qi W, Rao W, Sheng X, Shu W, Sutton J, Taft BR, Wang L, Zeng J, Zhang H, Zhang M, Zhao K, Lindvall MK, Bussiere DE. Structure-Guided Design of EED Binders Allosterically Inhibiting the Epigenetic Polycomb Repressive Complex 2 (PRC2) Methyltransferase. *J Med Chem*. 2016
34. Astle JM, Simpson LS, Huang Y, Reddy MM, Wilson R, Connell S, Wilson J, Kodadek T. Seamless bead to microarray screening: rapid identification of the highest affinity protein ligands from large combinatorial libraries. *Chem Biol*. 2010; 17(1):38–45. [PubMed: 20142039]
35. Lam KS, Salmon SE, Hersh EM, Hruby VJ, Kazmierski WM, Knapp RJ. A new type of synthetic peptide library for identifying ligand-binding activity. *Nature*. 1991; 354(6348):82–84. [PubMed: 1944576]
36. Doran TM, Gao Y, Mendes K, Dean S, Simanski S, Kodadek T. Utility of redundant combinatorial libraries in distinguishing high and low quality screening hits. *ACS Comb Sci*. 2014; 16(6):259–270. [PubMed: 24749624]
37. Gao Y, Kodadek T. Synthesis and screening of stereochemically diverse combinatorial libraries of peptide tertiary amides. *Chem Biol*. 2013; 20(3):360–369. [PubMed: 23521794]
38. Gao Y, Amar S, Pahwa S, Fields G, Kodadek T. Rapid lead discovery through iterative screening of one bead one compound libraries. *ACS Comb Sci*. 2014; 17(1):49–59. [PubMed: 25434974]
39. Qi X, Astle J, Kodadek T. Rapid identification of orexin receptor binding ligands using cell-based screening accelerated with magnetic beads. *Mol BioSyst*. 2010; 6(1):102–107. [PubMed: 20024071]

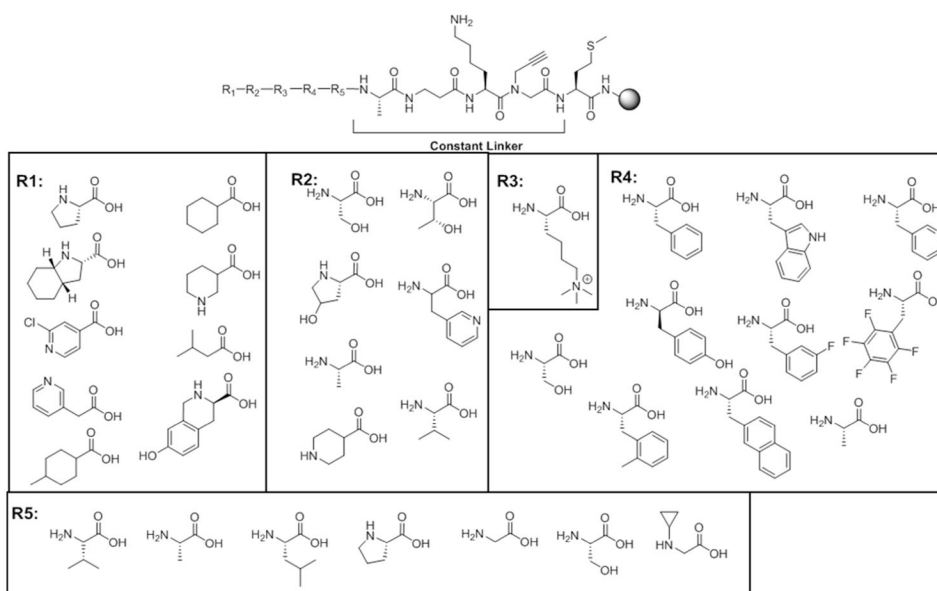


Figure 2. Compound 1-derivative library was designed to improve EED ligand potency by exploring a narrower region of chemical space at R1-R4 while also probing the tolerance of the R5 position to modification. The linker sequence provides distance between the library sequence and the solid support, and methionine was required for hit cleavage. Additionally, a lysine was included in the linker to promote proper display of the compounds on the bead surface³⁹.

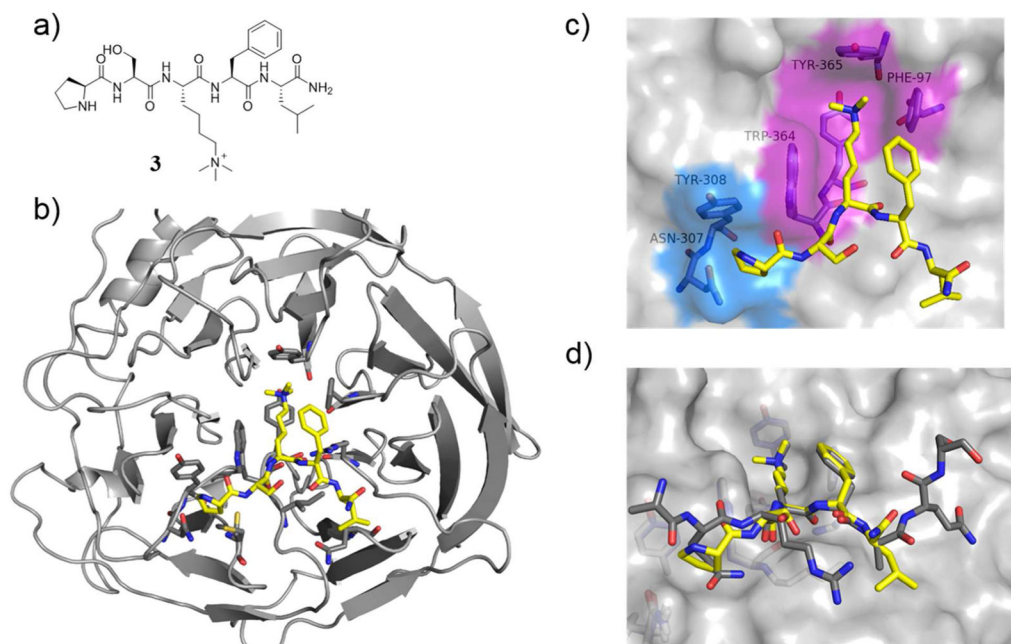


Figure 3.

a) Structure of compound **3**. The sequence was derived from the residues found to occur most frequently at each position in the redundant hits of the second generation combinatorial library. b) Co-crystal structure of compound **3** bound to EED (PDB 5TTW). c) The aromatic cage (magenta) and the adjacent hydrophobic pocket (blue) occupied by Kme3 and proline, respectively. The backbone of the serine residue bridges these two pockets while the side chain points to solvent. d) Alignment of Jarid2₁₁₀₋₁₂₀-K116me3 (dark grey) and compound **3** (yellow) structures bound to EED demonstrating the constrained proline ring (compound **3**) replaces glutamine (Jarid2₁₁₀₋₁₂₀-K116me3) and leucine (compound **3**) contacts a broader surface than alanine (Jarid2₁₁₀₋₁₂₀-K116me3).

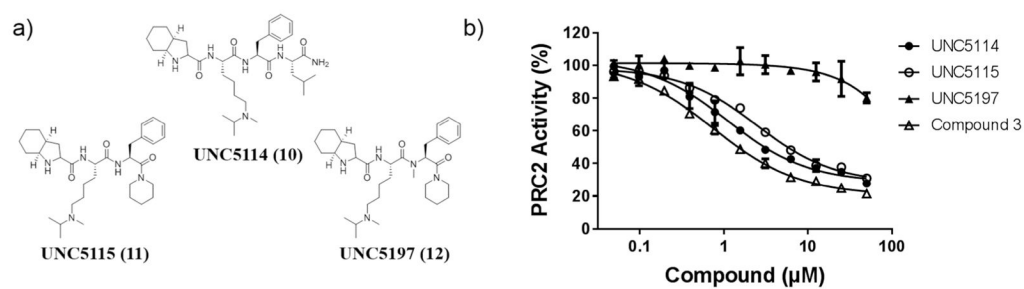


Figure 4.

a) Structures of UNC5114, UNC5115, and UNC5197. b) *In vitro* PRC2 catalytic scintillation proximity assay results for highest potency EED binders and the negative control demonstrate this series of ligands inhibits PRC2 methyltransferase activity.

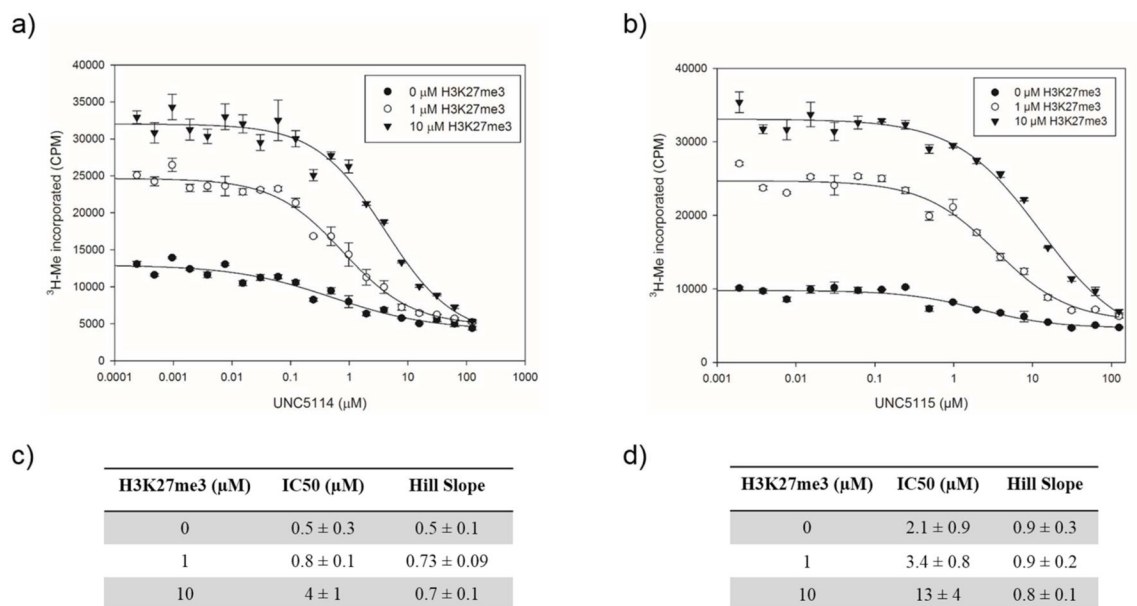


Figure 5. Effect of H3K27me3 competition at varying concentrations on a) UNC5114, and b) UNC5115 inhibition of PRC2 catalytic activity. IC₅₀ and Hill slope values for c) UNC5114 and d) UNC5115. Experiments were carried out in triplicate.

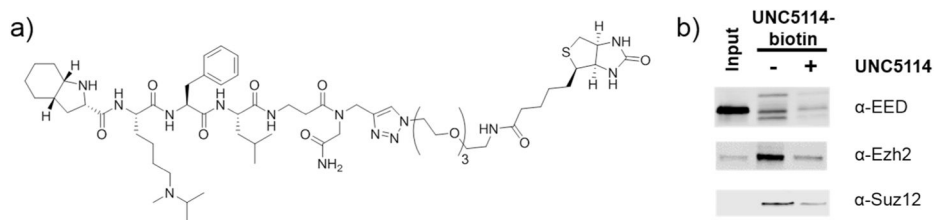


Figure 6. Chemiprecipitation of PRC2 core proteins. (A) Structure of C-terminally biotinylated derivative of UNC5114. (B) Western blot analysis indicating that UNC5114-biotin chemiprecipitates the intact PRC2 complex from PC-3 lysates with isolation of EED, Ezh2, and Suz12 (-). In the presence of soluble UNC5114, the ability of UNC5114-biotin to chemiprecipitate PRC2 is significantly reduced (+).

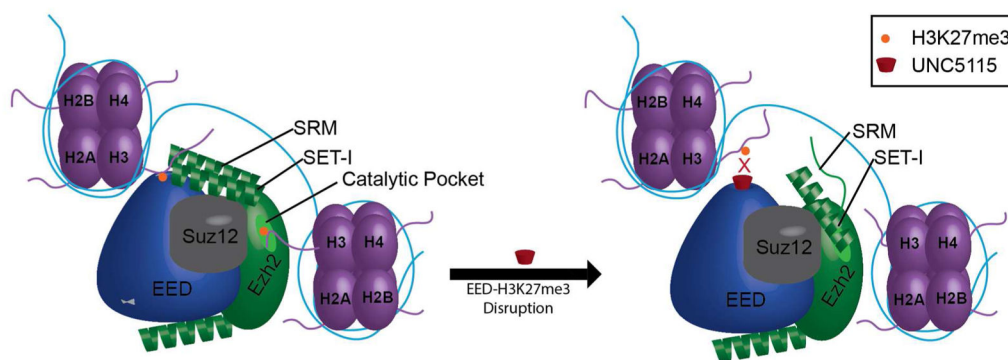
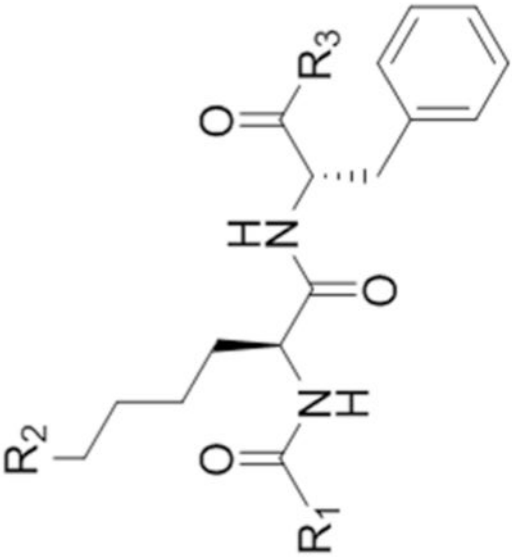
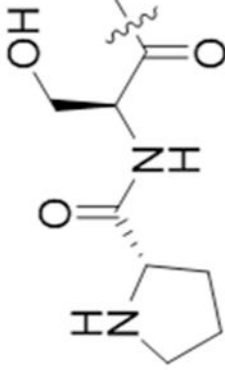
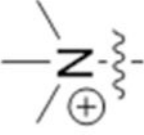
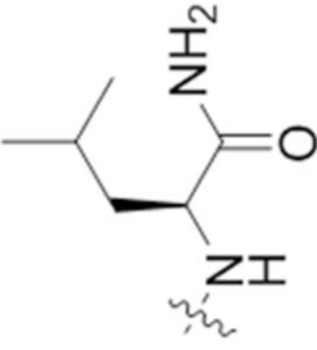


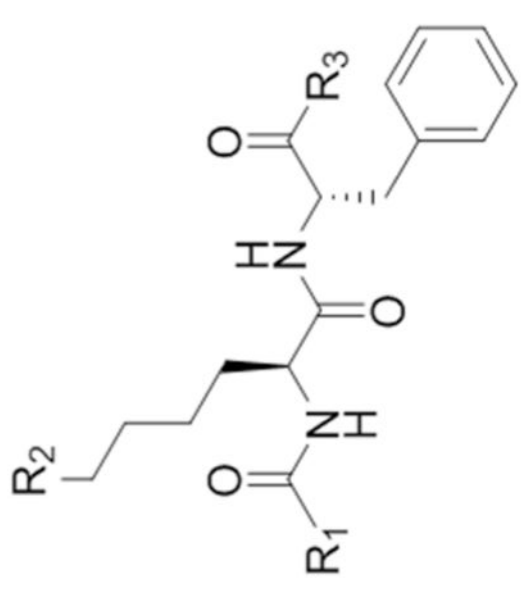
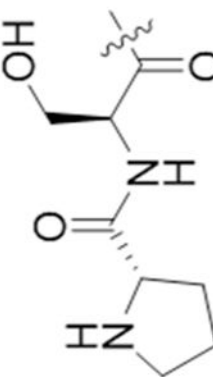
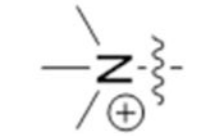
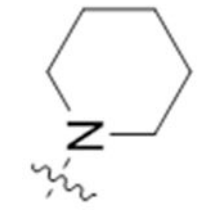
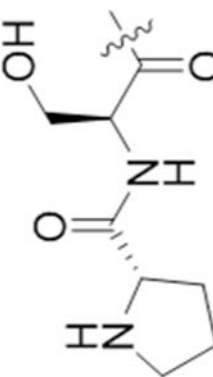
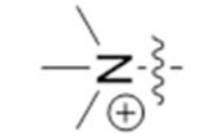
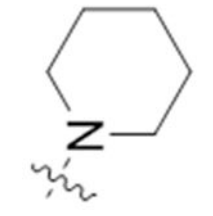
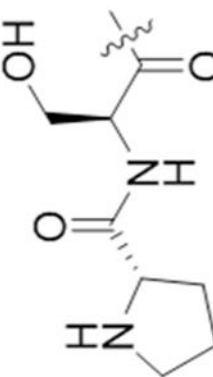
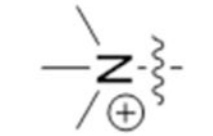
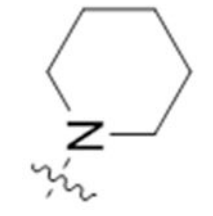
Figure 7. Model for allosteric inhibition of PRC2 catalytic activity. EED aromatic cage ligands prevent binding of activating H3K27me3 peptides and may disrupt the stabilization of the SRM helix which in turn fails to engage and stabilize the SET-I helix.

Table 1

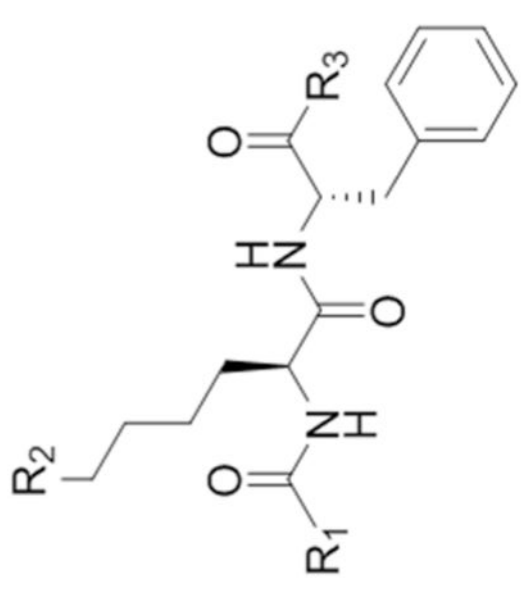
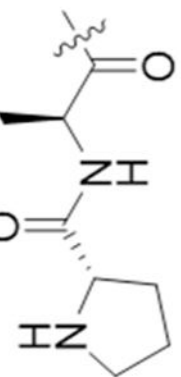
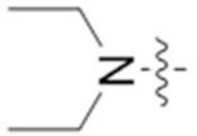
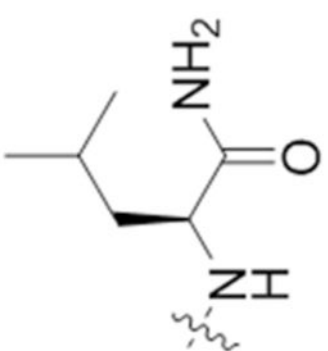
Exploration of N- and C-terminal Variations and Kme3 Replacements via FP.

	R ₁	R ₂	R ₃	IC ₅₀ (μM)
				14.78 ± 2.24

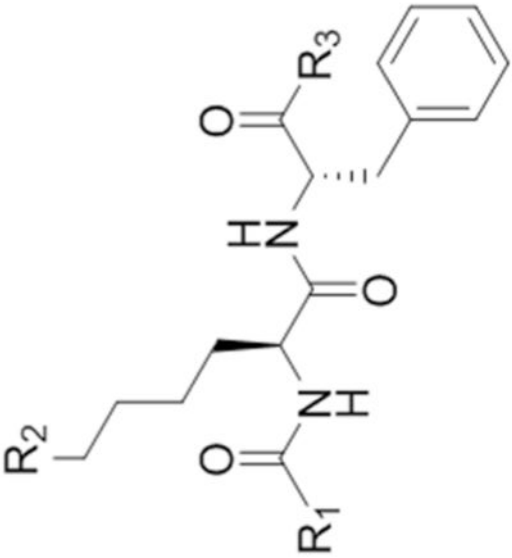
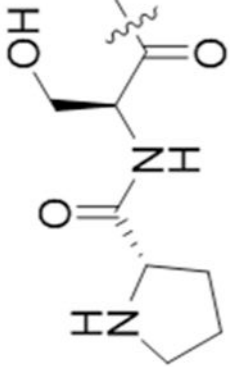
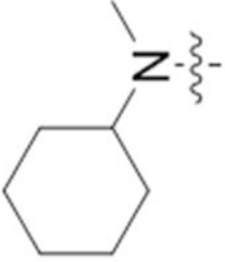
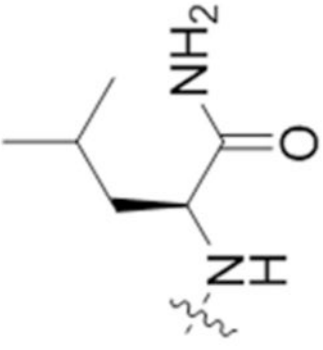
	R ₁	R ₂	R ₃	IC ₅₀ (μM)	1.65 ± 0.66	
						3

	IC_{50} (μM)	1.89 ± 0.51
R_1 	R_2 	R_3 
R_1 	R_2 	R_3 
R_1 	R_2 	R_3 

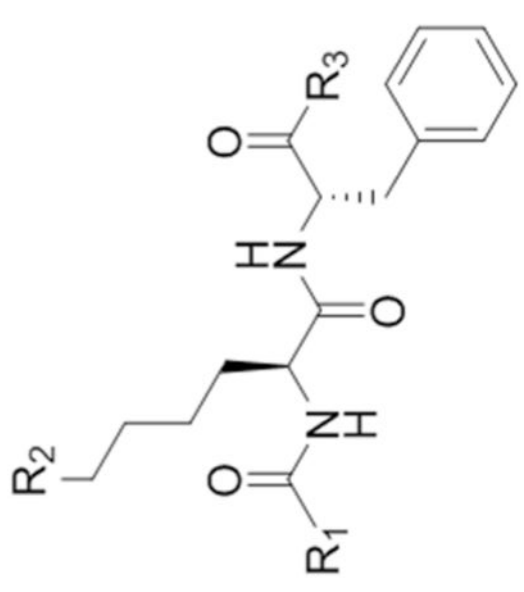
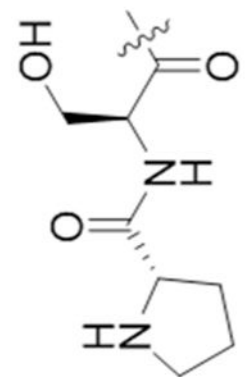
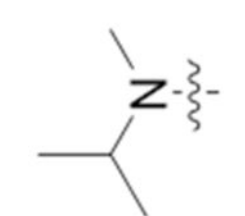
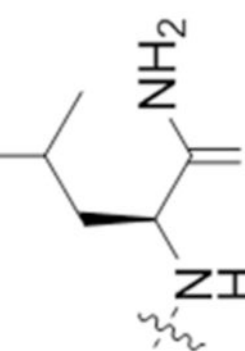
4

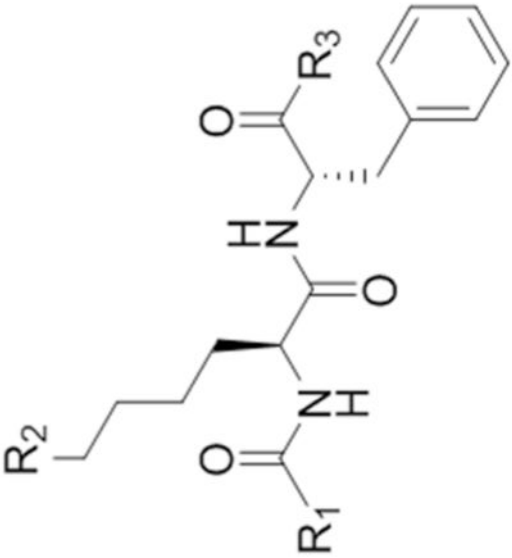
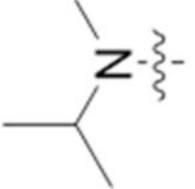
	R ₁	R ₂	R ₃	IC ₅₀ (μM)
 <p>The image shows a general chemical structure of a dipeptide derivative. It consists of two amino acid residues linked by a peptide bond. The first residue has a substituent R₁ on its nitrogen and a hydrogen on its alpha carbon. The second residue has a substituent R₂ on its alpha carbon and a substituent R₃ on its nitrogen. A benzyl group is attached to the alpha carbon of the second residue.</p>	 <p>Chemical structure for R₁: A pyrrolidine ring is attached to a chiral center. The chiral center is also bonded to a hydrogen atom and a hydroxyl group.</p>	 <p>Chemical structure for R₂: A diethylamino group (N(CH₂CH₃)₂) attached to a chiral center.</p>	 <p>Chemical structure for R₃: A 2-amino-3-methylbutanoate derivative attached to a chiral center. The amino group is shown in a zwitterionic form (NH₃⁺).</p>	<p>11.77 ± 8.95</p>

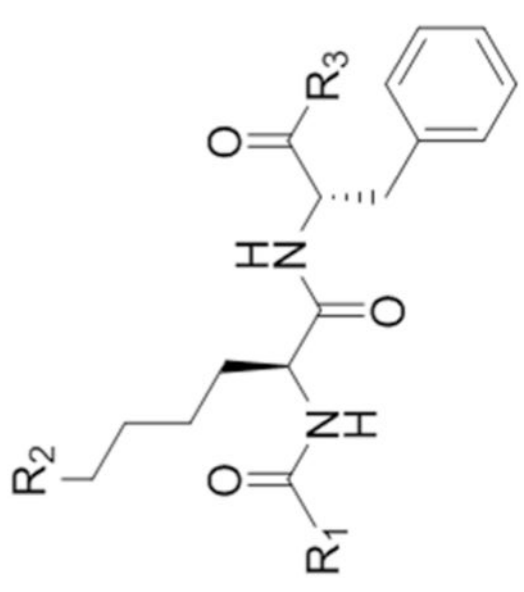



5

	<p>R₁</p>	<p>R₂</p>	<p>R₃</p>	<p>IC₅₀ (μM)</p>
				<p>>30</p>

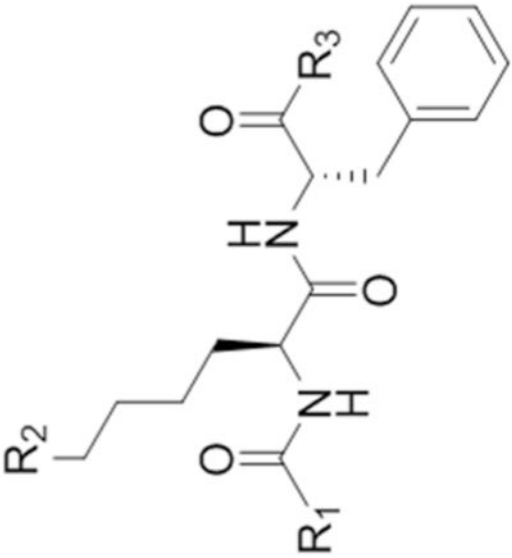
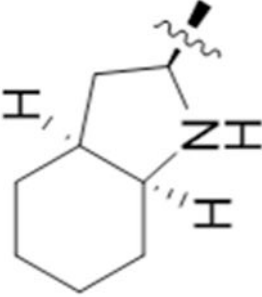
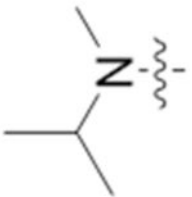
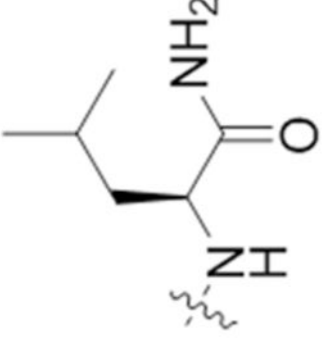
9

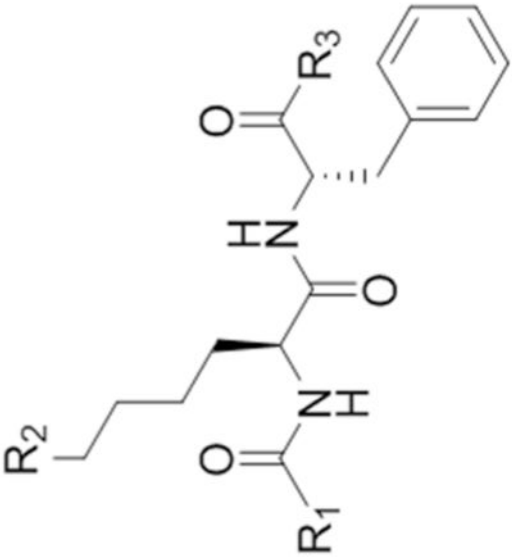
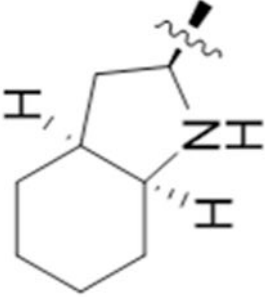
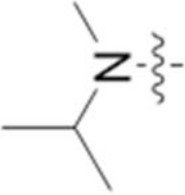
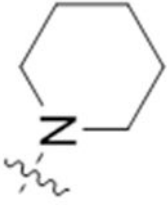
	R ₁	R ₂	R ₃	IC ₅₀ (μM)
 <p>The image shows a general chemical structure of a dipeptide derivative. It consists of two amino acid residues linked by a peptide bond. The first residue has a substituent R₁ on its alpha-carbon and an NH group. The second residue has a substituent R₂ on its alpha-carbon and an NH group. The side chain of the second residue is a benzyl group. The side chain of the first residue is a phenyl group. The structure is shown with stereochemistry: the R₁ group is on a wedge, the R₂ group is on a dash, and the benzyl group is on a dash.</p>	 <p>The structure for R₁ is a pyrrolidine ring attached to a chiral center. The chiral center is also bonded to a hydroxyl group (OH) and a carbonyl group (C=O).</p>	 <p>The structure for R₂ is an isopropyl group attached to a nitrogen atom. The nitrogen atom is also bonded to a methyl group and a wavy line representing a substituent.</p>	 <p>The structure for R₃ is a chiral center bonded to an amino group (NH₂), a methyl group, and a wavy line representing a substituent.</p>	<p>4.73 ± 1.66</p>

 <p>The image shows a general chemical structure of a tryptophan derivative. It consists of an indole ring system (R₁) attached to a chiral carbon atom. This carbon is also bonded to a hydrogen atom (wedge bond), an amide group (-NH-C(=O)-R₂), and another chiral carbon atom. This second chiral carbon is bonded to a hydrogen atom (dashed bond), a benzyl group (-CH₂-C₆H₅), and an amide group (-NH-C(=O)-R₃).</p>	R ₁	R ₂	R ₃	IC ₅₀ (μM)
8			 <p>The image shows a tryptophan derivative where the amide group (-NH-C(=O)-R₂) is replaced by a dimethylamino group (-N(CH₃)₂).</p>	>30

	R ₁	R ₂	R ₃	IC ₅₀ (μM)	
 <p>The general structure shows a piperazine ring substituted at the 4-position with a phenyl ring. The phenyl ring has a wavy line indicating a substituent. The piperazine ring is connected via an oxygen atom to a carbon atom, which is also bonded to a hydrogen atom and a nitrogen atom. This nitrogen atom is part of an amide group (-NH-C(=O)-R₁). The carbon atom is also bonded to a hydrogen atom and a nitrogen atom. This nitrogen atom is part of another amide group (-NH-C(=O)-R₂). The carbon atom is also bonded to a hydrogen atom and a nitrogen atom. This nitrogen atom is part of a third amide group (-NH-C(=O)-R₃). The carbon atom is also bonded to a hydrogen atom and a nitrogen atom. This nitrogen atom is part of a fourth amide group (-NH-C(=O)-R₃). The carbon atom is also bonded to a hydrogen atom and a nitrogen atom. This nitrogen atom is part of a fifth amide group (-NH-C(=O)-R₃).</p>	R ₁	R ₂	R ₃	 <p>The structure shows a piperazine ring substituted at the 4-position with a phenyl ring. The phenyl ring has a wavy line indicating a substituent. The piperazine ring is connected via an oxygen atom to a carbon atom, which is also bonded to a hydrogen atom and a nitrogen atom. This nitrogen atom is part of an amide group (-NH-C(=O)-R₁). The carbon atom is also bonded to a hydrogen atom and a nitrogen atom. This nitrogen atom is part of another amide group (-NH-C(=O)-R₂). The carbon atom is also bonded to a hydrogen atom and a nitrogen atom. This nitrogen atom is part of a third amide group (-NH-C(=O)-R₃). The carbon atom is also bonded to a hydrogen atom and a nitrogen atom. This nitrogen atom is part of a fourth amide group (-NH-C(=O)-R₃). The carbon atom is also bonded to a hydrogen atom and a nitrogen atom. This nitrogen atom is part of a fifth amide group (-NH-C(=O)-R₃).</p>	
			 <p>The structure shows a piperazine ring substituted at the 4-position with a phenyl ring. The phenyl ring has a wavy line indicating a substituent. The piperazine ring is connected via an oxygen atom to a carbon atom, which is also bonded to a hydrogen atom and a nitrogen atom. This nitrogen atom is part of an amide group (-NH-C(=O)-R₁). The carbon atom is also bonded to a hydrogen atom and a nitrogen atom. This nitrogen atom is part of another amide group (-NH-C(=O)-R₂). The carbon atom is also bonded to a hydrogen atom and a nitrogen atom. This nitrogen atom is part of a third amide group (-NH-C(=O)-R₃). The carbon atom is also bonded to a hydrogen atom and a nitrogen atom. This nitrogen atom is part of a fourth amide group (-NH-C(=O)-R₃). The carbon atom is also bonded to a hydrogen atom and a nitrogen atom. This nitrogen atom is part of a fifth amide group (-NH-C(=O)-R₃).</p>	 <p>The structure shows a piperazine ring substituted at the 4-position with a phenyl ring. The phenyl ring has a wavy line indicating a substituent. The piperazine ring is connected via an oxygen atom to a carbon atom, which is also bonded to a hydrogen atom and a nitrogen atom. This nitrogen atom is part of an amide group (-NH-C(=O)-R₁). The carbon atom is also bonded to a hydrogen atom and a nitrogen atom. This nitrogen atom is part of another amide group (-NH-C(=O)-R₂). The carbon atom is also bonded to a hydrogen atom and a nitrogen atom. This nitrogen atom is part of a third amide group (-NH-C(=O)-R₃). The carbon atom is also bonded to a hydrogen atom and a nitrogen atom. This nitrogen atom is part of a fourth amide group (-NH-C(=O)-R₃). The carbon atom is also bonded to a hydrogen atom and a nitrogen atom. This nitrogen atom is part of a fifth amide group (-NH-C(=O)-R₃).</p>	>30

9

 <p>General chemical structure of compound 10, featuring a bicyclic core (cyclohexane fused to a five-membered ring with an NH group). The structure is substituted with R₁, R₂, and R₃ groups. The R₁ group is attached to the nitrogen of the five-membered ring. The R₂ group is attached to the nitrogen of the adjacent amide group. The R₃ group is attached to the carbonyl carbon of the amide group. A phenyl ring is also attached to the amide group.</p>	R ₁	R ₂	R ₃	<p>IC₅₀ (μM)</p> <p>1.74 ± 0.78</p>	
<p>10 (UNC5114)</p>					

	R ₁	R ₂	R ₃	IC ₅₀ (μM)
 <p>General structure of compound 11 (UNC5115) showing substituents R₁, R₂, and R₃.</p>				3.87 ± 0.93

11 (UNC5115)

^a Average IC₅₀ values were calculated from 3–4 replicate runs. Error is reported as the standard error.